

*Physics beyond the Standard Model
from the study of weak interactions*



Sabin Stoica

*International Center for Advanced Training and Research in Physics
(CIFRA), Bucharest-Măgurele, Romania*

The image shows two logos side-by-side, separated by a vertical dotted line. On the left is the UNESCO logo, which consists of a classical building facade with the word 'UNESCO' in a bold, sans-serif font below it. Underneath the UNESCO logo is the text 'United Nations Educational, Scientific and Cultural Organization'. On the right is the CIFRA logo, which features a stylized 'C' containing a gear and a globe, followed by the letters 'IFRA' in a large, bold, blue font. Below the CIFRA logo is the text 'sous les auspices de l'UNESCO'. Underneath the CIFRA logo is the text 'Centre International de Formation et de Recherche Avancées en Physique subsidiary of NIMP'.

Outline

- ❖ Beta (BD) and double beta decay (DBD) processes
- ❖ Computation of the kinematic part of the decay rates: PSF, electron energy spectra and angular correlation
- ❖ Application to:
 - i) search of Lorentz invariance violation in $2\nu\beta\beta$ decay
 - ii) description of the EC processes
- ❖ Results and discussions
- ❖ Conclusions

Weak processes with electron/positron emission

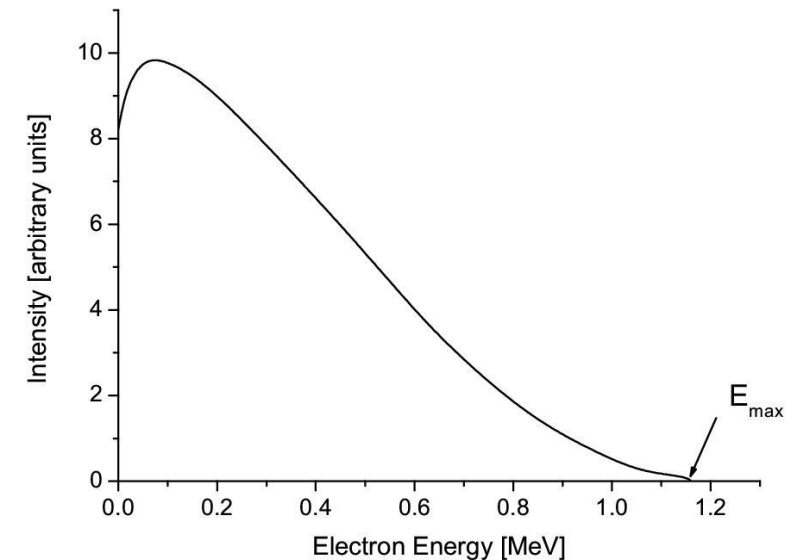
Beta decays



Beta decay.

Offers opportunities to explore several domains: nuclear structure, exotic nuclei; stellar processes, etc; beyond BSM: direct measurement of absolute ν mass; investigating deviations from the pure V-A theory; right-handed currents ; violation of Lorentz invariance through the analysis of electron spectra measurements; EC: applications in nuclear metrology and nuclear medicine; background characterization in DM&DBD experiments, etc.

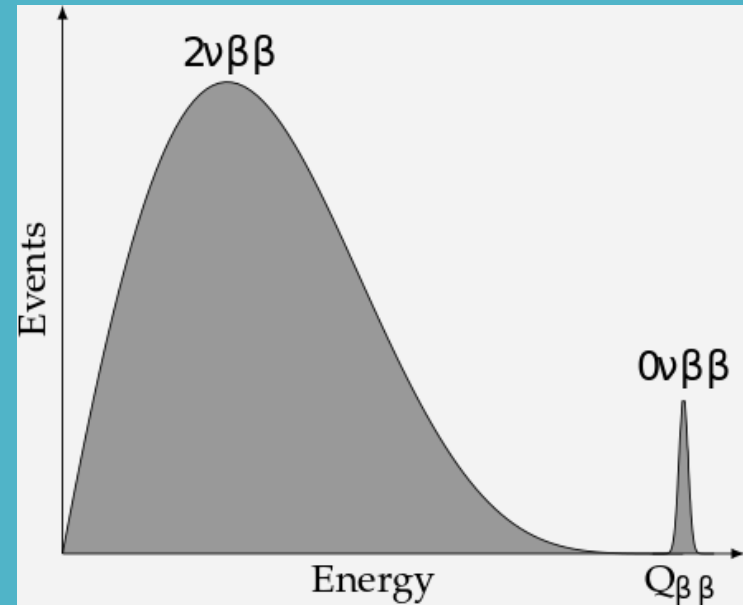
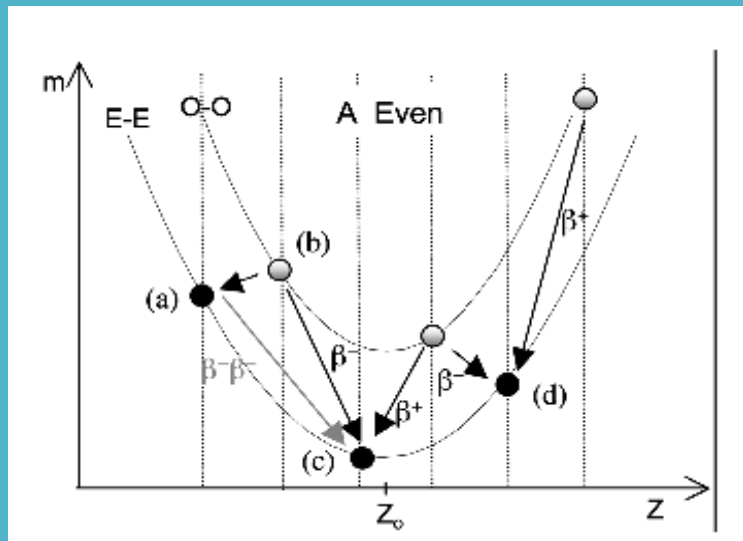
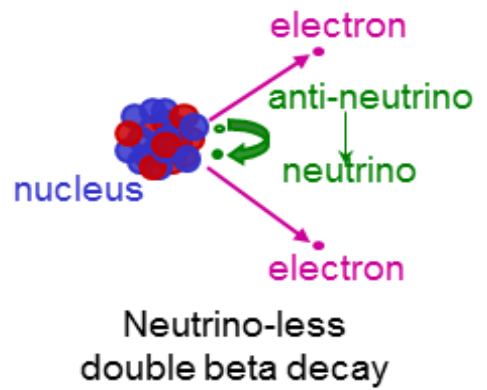
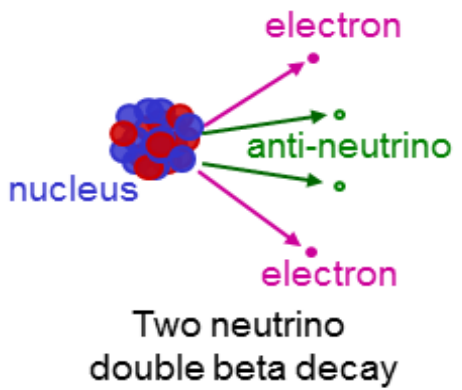
Transition	L	ΔI	$\Delta\pi$
Fermi	0	0	0
Gamow-Teller	0	0, 1	0
1st-forbidden (parity change)	1	0, 1, 2	1
2nd-forbidden (no parity change)	2	1, 2, 3	0
3rd-forbidden (parity change)	3	2, 3, 4	1
4th-forbidden (no parity change)	4	3, 4, 5	0



Double-beta decay modes

the rarest known radioactive decay
 measured until now, by which an e-e nucleus transforms into another e-e nucleus with the same mass but with its nuclear charge changed by two units. It occurs whenever single β decay can not occur due to energetical reasons or it is highly forbidden by angular momentum selection rules

- | | |
|----------------------|----------------------|
| $2\nu\beta^-\beta^-$ | $0\nu\beta^-\beta^-$ |
| $2\nu\beta^+\beta^+$ | $0\nu\beta^+\beta^+$ |
| $2\nu EC\beta^+$ | $0\nu EC\beta^+$ |
| $2\nu ECEC$ | $0\nu ECE$ |



Isotope	$Q_{\beta\beta}$ [MeV]	$T^{2\nu}$ [yr] [1]
^{48}Ca	4.272	$4.40 \times 10^{19}(\text{d})$
^{76}Ge	2.039	$1.65 \times 10^{21}(\text{d})$
^{82}Se	2.995	$9.20 \times 10^{19}(\text{d})$
^{96}Zr	3.350	$2.30 \times 10^{19}(\text{d})$
^{100}Mo	3.034	$7.10 \times 10^{18}(\text{d})$
^{116}Cd	2.814	$2.87 \times 10^{19}(\text{d})$
^{128}Te	0.866	$2.00 \times 10^{21}(\text{g})$
^{130}Te	2.527	$6.90 \times 10^{20}(\text{d}\&\text{g})$
^{136}Xe	2.458	$2.19 \times 10^{21}(\text{d})$
^{150}Nd	3.371	$8.20 \times 10^{18}(\text{d})$
^{238}U	1.450	$2.00 \times 10^{21}(\text{r})$
$^{235}\text{Ba}(2\nu ECEC)$	2.619	$\sim 1.0 \times 10^{21}(\text{g})$
$^{100}\text{Mo}-^{100}\text{Ru}(0_1)$	1.903	$6.70 \times 10^{20}(\text{d})$
$^{150}\text{Nd}-^{150}\text{Sm}(0_1)$	2.630	$1.20 \times 10^{20}(\text{d})$

DBD potential to explore BSM physics

Double-beta decay :

- Check of lepton number conservation ($\Delta L = 2$);
- Neutrino properties: Dirac or Majorana; limits on $\langle m_{\nu e} \rangle$
sterile $\nu_s \rightarrow$ limits on $\langle m_N \rangle$
neutrino mass hierarchy
- Distinguishing and constraining of different BSM scenarios for $0\nu\beta\beta$: Majoron existence, SUSY particles, L-R theories, \exists of RH currents
- Check of other symmetries: CP, Lorentz invariance

DBD lifetimes

$$[T_{1/2}^{2\nu}]^{-1} = G^{2\nu}(Q_{\beta\beta}, Z) \times g_A^4 \times |m_e c^2 M^{2\nu}|^2 \quad 2\nu\beta\beta$$

$$[T_{1/2}^{0\nu}]^{-1} = \sum_k [G^{0\nu}(Q_{\beta\beta}, Z) \times g_A^4 \times |M_k^{0\nu}|^2 \times \langle \eta_k \rangle] \quad 0\nu\beta\beta$$



$G^{(2,0)\nu}(E_0, Z)$ phase space factors (PSF)

$M^{(2,0)\nu}$ = nuclear matrix elements (NME)

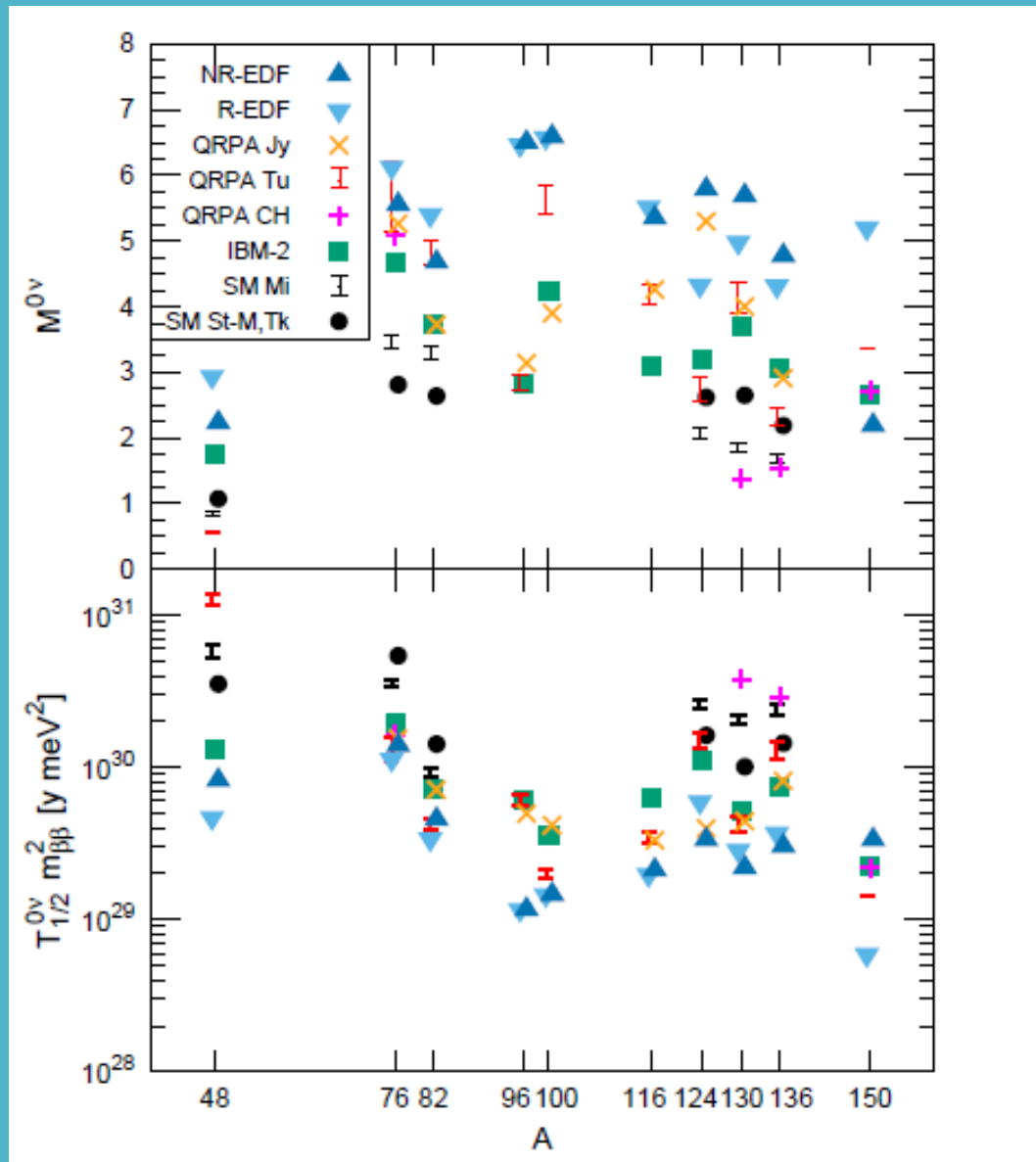
$$\sum_k M_k^{0\nu} = |M_{\nu}^{0\nu}|^2 \langle m_{\nu} \rangle^2 + |M_N^{0\nu}|^2 \langle m_N \rangle^2 + |M_{\lambda}^{0\nu}|^2 \langle \eta_{\lambda} \rangle^2 + |M_q^{0\nu}|^2 \langle \eta_q \rangle^2 + \dots$$

$\langle \eta_l \rangle$ = BSM parameter specific the $0\nu\beta\beta$ mechanism; g_A = axial-vector constant

Precise calculations of PSF and NME are needed to predict lifetimes, derive neutrino parameters, extract information on neutrino properties

$$M_{2\nu} = \sum_N \frac{\langle 0_F^+ || \tau^+ \sigma || 1_N^+ \rangle \langle 1_N^+ || \tau^+ \sigma || 0_I^+ \rangle}{\frac{1}{2}W_0 + E_N - E_I}$$

$$M^{0\nu} = M_{GT}^{0\nu} - \left(\frac{g_V}{g_A} \right)^2 M_F^{0\nu} + M_T^{0\nu}$$



Engel&Menendez-RPP2017

NME computation - a long standing problem

- Traditional methods give differences between NME values of up to 3-5 times and it's hard to compare and assess the correctness of the results, because is difficult to distinguish between errors/uncertainties due to different input parameters and shortcomings of the methods. Uncertainties in the NME values are further amplified, since they enter at the power of two in the inverse DBD lifetime formula.
- they each use empirical interactions that are not appropriate for other methods, and they each make ad-hoc assumptions about the short-range correlation effects on the transition.

Goal: to compute $0\nu\beta\beta$ NME with minimal model dependence and quantified theoretical uncertainty

- It is expected that chiral EFT combined with Lattice-QCD to specify the form of the decay operator determining the constants that multiply particular terms in the operator and ab-initio calculations to produce reliable NME with quantified uncertainties.

Current situation

There are NME calculations with modern no-core nuclear methods only for the lightest DBD isotopes ^{48}Ca , ^{76}Ge and ^{82}Se . Also, calculations with EFT combined with lattice QCD still face difficulties to provide the form of decay operator.

Statistical model (Horoi, Neacsu, Stoica, PRC2022, PRC2023; Horoi, Neacsu, Universe 2024)

for analysing the stability and distribution of the $0\nu\beta\beta$ NME calculated with ISM for ^{136}Xe , ^{48}Ca and ^{48}Se .

Goal: the stability of the NME values against small random changes of the TBME ($\pm 10\%$).

The calculations are performed using 3 independent effective Hamiltonians appropriate for each isotope.

(i) distribution of the NME values;

(ii) correlations of $0\nu\beta\beta$ NME with other observables (accessible experimentally): $2\nu\beta\beta$, GT transitions, excited states, occupancies, $B(E2)$; **in total 24 observables**

(iii) the theoretical ranges for each observables;

(iv) the shape of different distributions for each observables and starting Hamiltonians;

(iv) the weighted contributions from different starting Hamiltonians to the "optimal" distribution of the $0\nu\beta\beta$ NME;

(v) an "optimal" value of the $0\nu\beta\beta$ NME and its predicted probable range (theoretical error).

$\text{NME}(^{136}\text{Xe})$: (1.55 - 2.65) at 90\% CL with 1.95 mean value

$\text{NME}(^{48}\text{Ca})$: (0.45 - 0.65) at 90\% CL with 0.68 mean value

Calculation of the phase space factors for DBD

Topics of interest in this treatment are the energy and angular distributions of the emitted electrons, which are calculated by using exact Dirac wave functions with finite nuclear size and electron screening.

$$G_{2\nu}^{\beta\beta}(0^+ \rightarrow 0^+) = \frac{2\tilde{A}^2}{3 \ln 2 g_A^4 (m_e c^2)^2} \int_{m_e c^2}^{Q^{\beta\beta} + m_e c^2} d\epsilon_1 \int_{m_e c^2}^{Q^{\beta\beta} + 2m_e c^2 - \epsilon_1} d\epsilon_2 \int_0^{Q^{\beta\beta} + 2m_e c^2 - \epsilon_1 - \epsilon_2} d\omega_1 f_{11}^{(0)} w_{2\nu} (\langle K_N \rangle^2 + \langle L_N \rangle^2 + \langle K_N \rangle \langle L_N \rangle)$$

$$\frac{dG_{2\nu}^{(0)}}{d\epsilon_1}$$

single electron spectra

Single state dominance (summation over N reduces to one state and $\langle E_N \rangle = 1^+$)

$$\frac{dG_{2\nu}^{(0)}}{d(\epsilon_1 + \epsilon_2 - 2m_e c^2)}$$

summed energy electron spectra

Transitions to excited 2^+ states (single and summed energy electron spectra from transitions to g.s and to 2^+ states differ each other)

$$\alpha(\epsilon_1) = \frac{dG_{2\nu}^{(1)}/d\epsilon_1}{dG_{2\nu}^{(0)}/d\epsilon_1}$$

electron angular correlation

Mechanisms (for $0\nu\beta\beta$ – single electron spectra and angular correlation are different each other for light ν exchange mechanisms and RH contributions)

B-decay

$$\lambda_{ij} = \ln 2 \frac{f_{ij}(T, \rho, E_f)}{(ft)_{ij}}$$

$$f_{ij} = \int_1^{w_m} w \sqrt{w^2 - 1} (w_m - w)^2 F(\pm Z, w) (1 - G_{\mp}) dw$$

Computation of the kinetic part of BD & DBD

Electron wave functions and Fermi functions

essential ingredients to compute PSF, electron spectra and all other needed kinematic quantities

A

$$F^{NR}(Z_f, \epsilon) = \frac{2\pi\eta}{1 - e^{-2\pi\eta}}$$

$$\eta = \pm\alpha Z_f \epsilon / p,$$

Non-relativistic treatment
Primakov&Rosen RPP22(1959)

B

$$F_0(Z_f, \epsilon) = 4(2pR)^{2(\gamma-1)} e^{\pi y} \frac{|\Gamma(\gamma_k + iy)|^2}{[\Gamma(2\gamma + 1)]^2},$$

$$\gamma = \sqrt{1 - (\alpha Z_f)^2}, \quad y = \pm\alpha Z_f \epsilon / p$$

Relativistic treatment: solution of a Dirac equation in a point charge Coulomb potential
Suhonen&Civitarese, PR 301 (1998);
Doi&Kotani, PTP1985
FNS and screening effects were not taken into account.

C

$$F(Z_f, \epsilon) = \frac{f_1^2(\epsilon, R_A) + g_{-1}^2(\epsilon, R_A)}{2p^2}$$

Fermi function built up from the radial solution of a Dirac equation in a Coulomb-type potential
Kotila&Iachello, PRC85(2012);
Stoica&Mirea PRC88(2013); RRP63(2015)

D

electron wave functions are obtained with the DHFS method using a different Coulomb potential. More suitable for describing EC processes: additional atomic effects can be included; screening effect is taken into account

Nitescu, Stoica, Simkovic, PRC107(2023)

Table 1: PSF for $\beta^-\beta^-$ decays to final g.s.

Nucleus	$Q_{g.s.}^{\beta^-\beta^-}$ (MeV)	$G_{2\nu}^{\beta^-\beta^-}$ (g.s.) (10^{-21} yr $^{-1}$)				$G_{0\nu}^{\beta^-\beta^-}$ (g.s.) (10^{-15} yr $^{-1}$)			
		This work	[27]	[23, 24]	[26]	This work	[27]	[23, 24]	[26]
^{48}Ca	4.267	15536	15550	16200	16200	24.65	24.81	26.1	26.0
^{76}Ge	2.039	46.47	48.17	53.8	52.6	2.372	2.363	2.62	2.55
^{82}Se	2.996	1573	1596	1830	1740	10.14	10.16	11.4	11.1
^{96}Zr	3.349	6744	6816		7280	20.48	20.58		23.1
^{100}Mo	3.034	3231	3308	3860	3600	15.84	15.92	18.7	45.6
^{110}Pd	2.017	132.5	137.7			4.915	4.815		
^{116}Cd	2.813	2688	2764		2990	16.62	16.70		18.9
^{128}Te	0.8665	0.2149	0.2688	0.35	0.344	0.5783	0.5878	0.748	0.671
^{130}Te	2.528	1442	1529	1970	1940	14.24	14.22	19.4	16.7
^{136}Xe	2.458	1332	1433	2030	1980	14.54	14.58	19.4	17.7
^{150}Nd	3.371	35397	36430	48700	48500	61.94	63.03	85.9	78.4
^{238}U	1.144	98.51	14.57			32.53	33.61		

Stoica, Mirea, *Frontiers in Physics* **7** (2019)
S. Stoica, Mirea, *Phys. Rev. C* **88** (2013)
Mirea, Pahomi, *Stoica Rom.Rep.Phys.* **67**(2015)

Table 2 Majorana neutrino mass parameters together with the other components of the $0\nu\beta\beta$ decay halftimes: the $Q_{\beta\beta}$ values, the experimental lifetimes limits, the phase space factors and the nuclear matrix elements.

	$Q_{\beta\beta}$ [MeV]	$T_{exp}^{0\nu\beta\beta}$ [yr]	$G^{0\nu\beta\beta}$ [yr $^{-1}$]	$M^{0\nu\beta\beta}$	$\langle m_\nu \rangle$ [eV]
^{48}Ca	4.272	$> 5.8 \cdot 10^{22}$ [52]	2.46E-14	0.81-0.90	$< [15.0 - 16.7]$
^{76}Ge	2.039	$> 2.1 \cdot 10^{25}$ [38]	2.37E-15	2.81-6.16	$< [0.37 - 0.82]$
^{82}Se	2.995	$> 3.6 \cdot 10^{23}$ [53]	1.01E-14	2.64-4.99	$< [1.70 - 3.21]$
^{96}Zr	3.350	$> 9.2 \cdot 10^{21}$ [54]	2.05E-14	2.19-5.65	$< [6.59 - 17.0]$
^{100}Mo	3.034	$> 1.1 \cdot 10^{24}$ [53]	1.57E-14	3.93-6.07	$< [0.64 - 0.99]$
^{116}Cd	2.814	$> 1.7 \cdot 10^{23}$ [56]	1.66E-14	3.29-4.79	$< [2.00 - 2.92]$
^{130}Te	2.527	$> 2.8 \cdot 10^{24}$ [57]	1.41E-14	2.65-5.13	$< [0.50 - 0.97]$
^{136}Xe	2.458	$> 1.6 \cdot 10^{25}$ [39]	1.45E-14	2.19-4.20	$< [0.25 - 0.48]$
^{150}Nd	3.371	$> 1.8 \cdot 10^{22}$ [55]	6.19E-14	1.71-3.16	$< [4.84 - 8.95]$

[23] M. Doi, T. Kotani and E. Takasugi, *Prog. Theor. Phys. Suppl.* **83**, 1 (1985).

[24] M. Doi and T. Kotani, *Prog. Theor. Phys.* **87**, 1207 (1992); *ibidem* **89**, 139 (1993).

[26] J. Suhonen and O. Civitarese, *Phys. Rep.* **300**, 123 (1998).

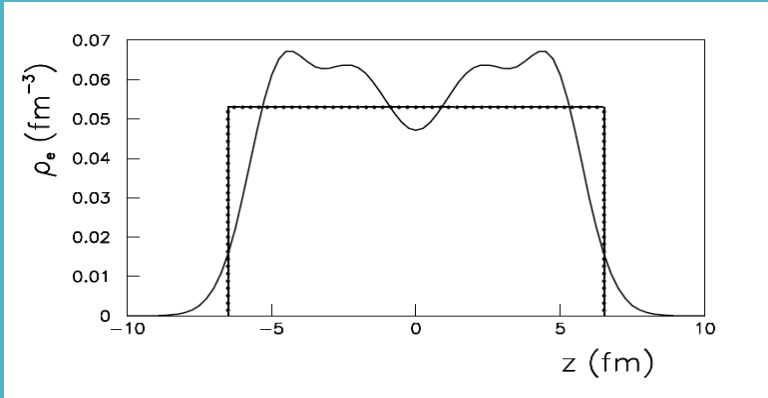
[27] J. Kotila and F. Iachello, *Phys. Rev. C* **85**, 034316 (2012).

$$\frac{dg_{\kappa}(\epsilon, r)}{dr} = -\frac{\kappa}{r}g_{\kappa}(\epsilon, r) + \frac{\epsilon - V + m_e c^2}{c\hbar}f_{\kappa}(\epsilon, r)$$

$$\frac{df_{\kappa}(\epsilon, r)}{dr} = -\frac{\epsilon - V - m_e c^2}{c\hbar}g_{\kappa}(\epsilon, r) + \frac{\kappa}{r}f_{\kappa}(\epsilon, r)$$

$$V(Z, r) = \begin{cases} -\frac{Z\alpha\hbar c}{r}, & r \geq R_A \\ -Z(\alpha\hbar c) \left(\frac{3-(r/R_A)^2}{2R_A} \right), & r < R_A \end{cases}$$

$$\frac{d^2\phi}{dx^2} = \frac{\phi^{3/2}}{\sqrt{x}}$$



$$\rho_e(\vec{r}) = \sum (2j_i + 1) v_i^2 |\psi_i(\vec{r})|^2$$

$$V(r) = \alpha\hbar c \int \frac{\rho_e(\vec{r}')}{|\vec{r} - \vec{r}'|} d\vec{r}'$$

$$f_{11}^{(0)} = |f^{-1-1}|^2 + |f_{11}|^2 + |f_1^{-1}|^2 + |f_1^{-1}|^2$$

$$f^{-1-1} = g_{-1}(\epsilon_1)g_{-1}(\epsilon_2); f_{11} = f_1(\epsilon_1)f_1(\epsilon_2),$$

$$f_1^{-1} = g_{-1}(\epsilon_1)f_1(\epsilon_2); f_1^{-1} = f_1(\epsilon_1)g_1(\epsilon_2)$$

Fermi functions from exact electron w.f. obtained as solutions of a Dirac equation with Coulomb-type potential built with a realistic proton density in nucleus, with inclusion of FNS and screening effects

Phase space for $2\nu\beta\beta$

$$G^{2\nu} = C_1 \int_0^Q d\epsilon_1 \int_0^{Q-\epsilon_1} d\epsilon_2 \int_0^{Q-\epsilon_1-\epsilon_2} d\omega_1 \\ \times F(Z_f, \epsilon_1) F(Z_f, \epsilon_2) \sqrt{\epsilon_1(\epsilon_1 + 2)}(\epsilon_1 + 1) \sqrt{\epsilon_2(\epsilon_2 + 2)}(\epsilon_2 + 1) \\ \times \omega_1^2 (Q - \epsilon_1 - \epsilon_2 - \omega_1)^2 (\langle K_N \rangle^2 + \langle L_N \rangle^2 + \langle K_N \rangle \langle L_N \rangle)$$

$$C_1 = (\tilde{A}^2 G_F^4 |V_{ud}|^4 m_e^9) / (96\pi^7 \ln 2)$$

$$\langle K_N \rangle = \frac{1}{\epsilon_1 + \omega_1 + \langle E_N \rangle - E_I} + \frac{1}{\epsilon_2 + \omega_2 + \langle E_N \rangle - E_I}$$

$$\langle L_N \rangle = \frac{1}{\epsilon_1 + \omega_2 + \langle E_N \rangle - E_I} + \frac{1}{\epsilon_2 + \omega_1 + \langle E_N \rangle - E_I}$$

$$\langle K_N \rangle \simeq \langle L_N \rangle \simeq \frac{2}{E_I - \langle E_N \rangle - (Q/2 + 1)}$$

Lorentz invariance violation in weak decays

- The general framework characterizing LIV is the Standard Model Extension (SME).
- In minimal SME (operators dimension ≤ 4) there are operators that couples to ν_s and affect ν flavor oscillations, ν velocity or ν phase spaces (β , $\beta\beta$ decays).
- First LIV searches in the ν sector were perform in ν oscillation experiments.
- LIV can now be also investigated in β and $\beta\beta$ decays by a precise analysis of the electron spectra.
- Since 2016 deviations to Lorentz symmetry began to be also investigated in DBD experiments: *EXO (PRD93-2016)*, *GERDA (arXiv22)*, *AURORA (PRD98-2018)*, *NEMO3 (EPJC79-2019)*, *CUPIDO (PRD100-2019)*, *CUORE (Front.Phys.2019)*.
- There is a q -independent component of the so-called counter-shaded operator, which doesn't affect the ν oscillations, and hence can not be detected in ν oscillation experiments, but can affect the electron spectra of $2\nu\beta\beta$ decay, namely: the summed energy spectra of electrons, or single energy spectra of electrons and electron angular correlation (the last can be investigated in experiments with tracking systems for the individual electrons).
- In the absence of observation of LIV deviations one can constrain the $\hat{a}_{of}^{(3)}$ coefficient that governs the isotropic (like-time) component of the counter-shaded operator.

The coupling of the neutrino to the counter-shaded operator modifies the neutrino momentum :

$$q^\alpha(\omega, \mathbf{q}) \rightarrow q^\alpha(\omega, \mathbf{q} + \mathbf{a}_{\text{of}}^{(3)} + \dot{\mathbf{a}}_{\text{of}}^{(3)} \mathbf{q}/q)$$

This, further, modifies the $2\nu\beta\beta$ transition amplitude, so the decay rate can be written as a sum of the standard term and a perturbation due to $LV\beta\beta$ (J.S. Diaz, PRD89(2014))

$$\Gamma^{(2\nu)} = \Gamma_0^{(2\nu)} + d\Gamma^{(2\nu)}$$

$$\Gamma_0^{(2\nu)} = G_0^{2\nu}(E_0, Z) \times g_A^4 \times |m_e c^2 M^{2\nu}|^2$$

$$d\Gamma^{(2\nu)} = dG_0^{2\nu}(E_0, Z) \times g_A^4 \times |m_e c^2 M^{2\nu}|^2$$

$$G_0^{2\nu} = C \int_0^Q d\varepsilon_1 F(Z, \varepsilon_1) [\varepsilon_1(\varepsilon_1 + 2)]^{1/2} (\varepsilon_1 + 1) \int_0^{Q-\varepsilon_1} d\varepsilon_2 F(Z, \varepsilon_2) [\varepsilon_2(\varepsilon_2 + 2)]^{1/2} (\varepsilon_2 + 1)(Q - \varepsilon_1 - \varepsilon_2)^5$$

$$dG^{2\nu} = 10\dot{\mathbf{a}}_{\text{of}}^{(3)} C \int_0^Q d\varepsilon_1 F(Z, \varepsilon_1) [\varepsilon_1(\varepsilon_1 + 2)]^{1/2} (\varepsilon_1 + 1) \int_0^{Q-\varepsilon_1} d\varepsilon_2 F(Z, \varepsilon_2) [\varepsilon_2(\varepsilon_2 + 2)]^{1/2} (\varepsilon_2 + 1)(Q - \varepsilon_1 - \varepsilon_2)^4$$

$$C = G_F^4 |V_{ud}|^4 m_e / 240\pi^7 \quad t_{1,2} = \varepsilon_{1,2} - 1;$$

$$F^{\text{NR}}(Z, \varepsilon) = 2\pi\eta / (1 - e^{-2\pi\eta})$$

Formalism for Lorentz invariant violation in DBD

Nitorescu, Ghinescu, Mirea, Stoica, JPG 47(2020)
Nitorescu, Ghinescu, Stoica, PRD103 (2021)
Ghinescu, Nitorescu, Stoica, PRD105(2022)

$$\Gamma_{\text{SME}} = \Gamma_{\text{SM}} + \delta\Gamma$$

Differential rate for $2\nu\beta\beta$ decay for ground states to ground states transitions

$$d\Gamma^{2\nu} = [\mathcal{A}^{2\nu} + \mathcal{B}^{2\nu} \cos \theta_{12}] w^{2\nu} d\omega_1 d\varepsilon_1 d\varepsilon_2 d(\cos \theta_{12})$$

$$w_{\text{SM}}^{2\nu} = \frac{g_A^4 G_F^4 |V_{ud}|^4}{64\pi^7} \omega_1^2 \omega_2^2 p_1 p_2 \varepsilon_1 \varepsilon_2$$

$$\begin{aligned} \mathcal{A}^{2\nu} &= \frac{1}{4} a(\varepsilon_1, \varepsilon_2) |M_{2\nu}|^2 \tilde{A}^2 \\ &\times \left[(\langle K_N \rangle + \langle L_N \rangle)^2 + \frac{1}{3} (\langle K_N \rangle - \langle L_N \rangle)^2 \right] \\ \mathcal{B}^{2\nu} &= \frac{1}{4} b(\varepsilon_1, \varepsilon_2) |M_{2\nu}|^2 \tilde{A}^2 \\ &\times \left[(\langle K_N \rangle + \langle L_N \rangle)^2 - \frac{1}{9} (\langle K_N \rangle - \langle L_N \rangle)^2 \right] \end{aligned}$$

ε, ω = electron and neutrino energies;
 p = electron momenta; θ = angle between electrons;
 K, N = kinematic factors

$$\begin{aligned} \langle K_N \rangle &= \frac{1}{\varepsilon_1 + \omega_1 + \langle E_N \rangle - E_I} + \frac{1}{\varepsilon_2 + \omega_2 + \langle E_N \rangle - E_I} \\ \langle L_N \rangle &= \frac{1}{\varepsilon_1 + \omega_2 + \langle E_N \rangle - E_I} + \frac{1}{\varepsilon_2 + \omega_1 + \langle E_N \rangle - E_I} \end{aligned}$$

$$\frac{d\Gamma_{\text{SM}}^{2\nu}}{d(\cos \theta_{12})} = \frac{1}{2} \Gamma_{\text{SM}}^{2\nu} [1 + \kappa_{\text{SM}}^{2\nu} \cos \theta_{12}]$$

$$\kappa_{\text{SM}}^{2\nu} = \frac{\Lambda_{\text{SM}}^{2\nu}}{\Gamma_{\text{SM}}^{2\nu}}$$

angular correlation coefficient

$$\frac{\Gamma_{\text{SM}}^{2\nu}}{\ln 2} = g_A^4 |m_e M_{2\nu}|^2 G_{\text{SM}}^{2\nu}, \quad \frac{\Lambda_{\text{SM}}^{2\nu}}{\ln 2} = g_A^4 |m_e M_{2\nu}|^2 H_{\text{SM}}^{2\nu}$$

$$d^3 q = 4\pi \omega^2 d\omega \quad \rightarrow$$

$$d^3 q = 4\pi (\omega^2 + 2\omega a_{\text{of}}^{(3)}) d\omega$$

$$\Gamma_{\text{SME}} = \Gamma_{\text{SM}} + \delta\Gamma$$

$$\Gamma_{\text{SME}}^{2\nu} = \Gamma_{00}^{2\nu} + \Gamma_{01}^{2\nu} + \Gamma_{10}^{2\nu}, \quad \Lambda_{\text{SME}}^{2\nu} = \Lambda_{00}^{2\nu} + \Lambda_{01}^{2\nu} + \Lambda_{10}^{2\nu}$$

$$G_{\text{SME}} = G_{\text{SM}} + \delta G, \\ H_{\text{SME}} = H_{\text{SM}} + \delta H$$

$$\frac{d\Gamma_{\text{SME}}^{2\nu}}{d(\cos \theta_{12})} = \frac{1}{2} \Gamma_{\text{SME}}^{2\nu} [1 + \kappa_{\text{SME}}^{2\nu} \cos \theta_{12}]$$

$$\kappa_{\text{SME}}^{2\nu} = \frac{\Lambda_{\text{SME}}^{2\nu}}{\Gamma_{\text{SME}}^{2\nu}}$$

$$\delta G^{2\nu} = \frac{2G_{10}^{2\nu}}{a_{\text{of}}^{(3)}}, \quad \delta H^{2\nu} = \frac{2H_{10}^{2\nu}}{a_{\text{of}}^{(3)}}$$

$$\frac{d\Gamma_{\text{SME}}^{2\nu}}{dK} = C \frac{dG_{00}^{2\nu}}{dK} (1 + \overset{\circ}{a}_{\text{of}}^{(3)} \chi^{(+)}(K))$$

$$\chi^{(+)} = \frac{d(\delta G^{2\nu})}{dK} / \frac{dG_{00}^{2\nu}}{dK}$$

$$\frac{d\Gamma_{\text{SME}}^{2\nu}}{d\varepsilon_1} = C \frac{dG_{00}^{2\nu}}{d\varepsilon_1} (1 + \overset{\circ}{a}_{\text{of}}^{(3)} \chi^{(1)}(\varepsilon_1))$$

$$\chi^{(1)} = \frac{d(\delta G^{2\nu})}{d\varepsilon_1} / \frac{dG_{00}^{2\nu}}{d\varepsilon_1}$$

$$\frac{d\Gamma_{\text{SM}}}{d\varepsilon_1 d(\cos \theta_{12})} = C \frac{dG_{\text{SM}}}{d\varepsilon_1} [1 + \alpha_{\text{SM}} \cos \theta_{12}]$$

$$\alpha_{\text{SM}} \equiv (dH_{00}^{2\nu}/d\varepsilon_1) / (dG_{00}^{2\nu}/d\varepsilon_1)$$

$$\frac{d\Gamma_{\text{SME}}}{d\varepsilon_1 d(\cos \theta_{12})} = C \frac{dG_{\text{SM}}}{d\varepsilon_1} \times \left[1 + \overset{\circ}{a}_{\text{of}}^{(3)} \chi^{(1)}(\varepsilon_1) + \left(\alpha_{\text{SM}} + \overset{\circ}{a}_{\text{of}}^{(3)} \frac{d(\delta H)/d\varepsilon_1}{dG_{\text{SM}}/d\varepsilon_1} \right) \cos \theta_{12} \right]$$

$$\alpha_{\text{SME}} = \alpha_{\text{SM}} + \overset{\circ}{a}_{\text{of}}^{(3)} \frac{d(\delta H^{2\nu})/d\varepsilon_1}{dG_{00}^{2\nu}/d\varepsilon_1}$$

$$\left\{ \begin{array}{l} G_{\text{SM}} \\ \delta G \end{array} \right\} = \frac{\tilde{A}^2 G_F^2 |V_{\text{ud}}|^2 m_e^9}{96\pi^7 \ln 2} \frac{1}{m_e^{11}} \int_{m_e}^{E_I - E_F - m_e} d\varepsilon_1 \varepsilon_1 p_1 \int_{m_e}^{E_I - E_F - \varepsilon_1} d\varepsilon_2 \varepsilon_2 p_2$$

$$\times \int_0^{E_I - E_F - \varepsilon_1 - \varepsilon_2} d\omega_1 \omega_2^2 a(\varepsilon_1, \varepsilon_2) [\langle K_N \rangle^2 + \langle L_N \rangle^2 + \langle K_N \rangle \langle L_N \rangle] \left\{ \begin{array}{l} \omega_1^2 \\ 4\overset{\circ}{a}_{\text{of}}^{(3)} \omega_1 \end{array} \right\},$$

$$\left\{ \begin{array}{l} H_{\text{SM}} \\ \delta H \end{array} \right\} = \frac{\tilde{A}^2 G_F^2 |V_{\text{ud}}|^2 m_e^9}{96\pi^7 \ln 2} \frac{1}{m_e^{11}} \int_{m_e}^{E_I - E_F - m_e} d\varepsilon_1 \varepsilon_1 p_1 \int_{m_e}^{E_I - E_F - \varepsilon_1} d\varepsilon_2 \varepsilon_2 p_2$$

$$\times \int_0^{E_I - E_F - \varepsilon_1 - \varepsilon_2} d\omega_1 \omega_2^2 b(\varepsilon_1, \varepsilon_2) \left[\frac{2}{3} \langle K_N \rangle^2 + \frac{2}{3} \langle L_N \rangle^2 + \frac{5}{3} \langle K_N \rangle \langle L_N \rangle \right] \left\{ \begin{array}{l} \omega_1^2 \\ 4\overset{\circ}{a}_{\text{of}}^{(3)} \omega_1 \end{array} \right\}$$

$$\frac{dG_{2\nu}^{(0)}}{d(\varepsilon_1 + \varepsilon_2 - 2m_e c^2)}$$

$$\frac{dG_{2\nu}^{(0)}}{d\varepsilon_1}$$

$$\alpha(\varepsilon_1) = \frac{dG_{2\nu}^{(1)}/d\varepsilon_1}{dG_{2\nu}^{(0)}/d\varepsilon_1}$$

$$\delta G^{2\nu} = 10\overset{\circ}{a}_{\text{of}}^{(3)} C_2 \int_0^Q d\varepsilon_1 \int_0^{Q-\varepsilon_1} d\varepsilon_2 \int_0^{Q-\varepsilon_1-\varepsilon_2} d\omega_1$$

$$\times F(Z_f, \varepsilon_1) F(Z_f, \varepsilon_2) \sqrt{\varepsilon_1(\varepsilon_1 + 2)}(\varepsilon_1 + 1) \sqrt{\varepsilon_2(\varepsilon_2 + 2)}(\varepsilon_2 + 1)$$

$$\times \omega_1 (Q - \varepsilon_1 - \varepsilon_2 - \omega_1)^2 (\langle K_N \rangle^2 + \langle L_N \rangle^2 + \langle K_N \rangle \langle L_N \rangle)$$

Results and discussions

Summed energy spectra of electrons in DBD

Summed energy spectra of electrons in the approximations A, B and C

A= NR approx. is inadequate in precise electron spectra analyses

B = approx. (analytical Fermi function); non-inclusion of FNS and screening effects: differences up to 30% as compared with “exact” Fermi function

C = exact Fermi functions, screening effect, “realistic” Coulomb-type potential

Nitescu, Ghinescu, Mirea, Stoica, JPG 47, 055112 (2020)

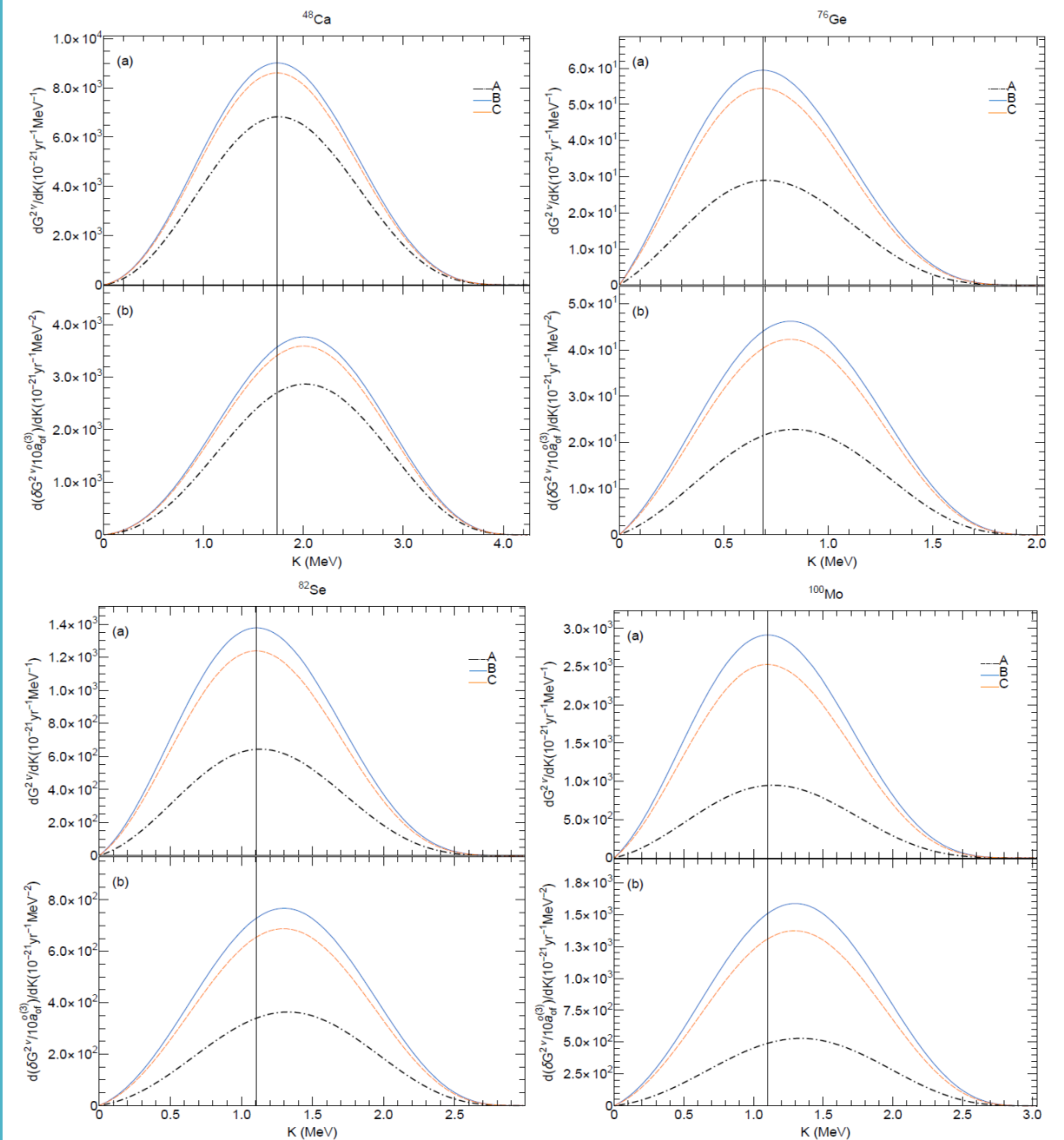


Figure 1. Summed energy spectra of electrons in the standard $2\nu\beta\beta$ decay (a) and their deviations due to LIV (b) for the nuclei ^{48}Ca , ^{76}Ge , ^{82}Se and ^{100}Mo .

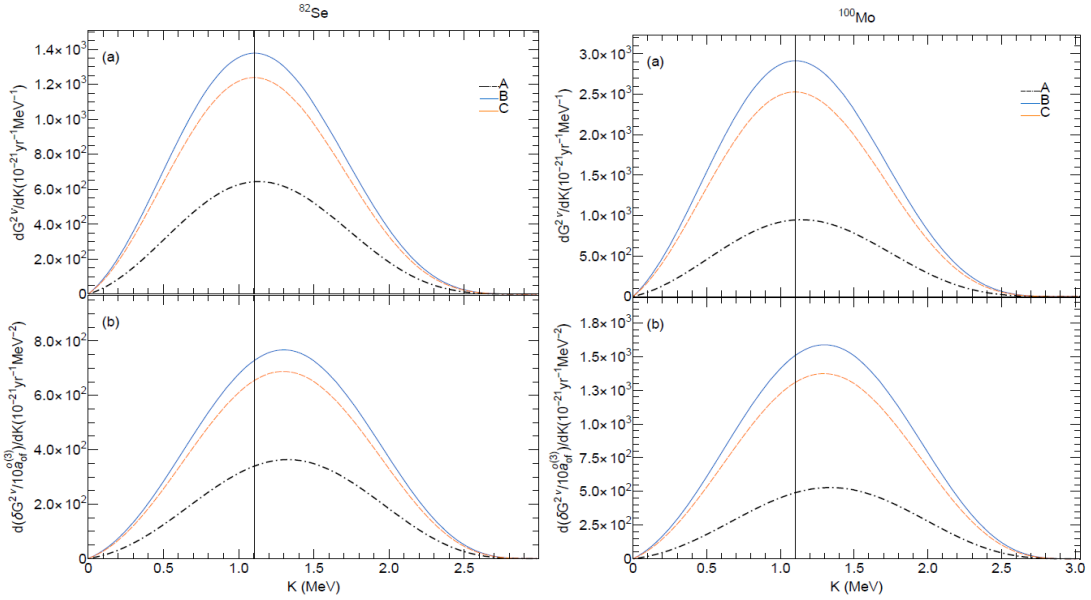
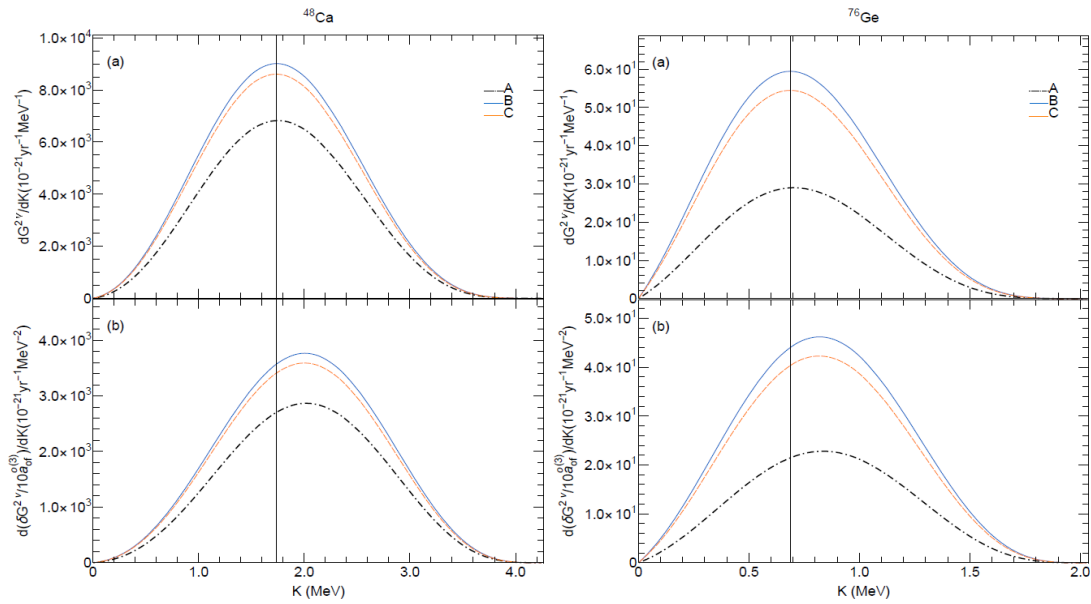


Figure 1. Summed energy spectra of electrons in the standard $2\nu\beta\beta$ decay (a) and their deviations due to LIV (b) for the nuclei ^{48}Ca , ^{76}Ge , ^{82}Se and ^{100}Mo .

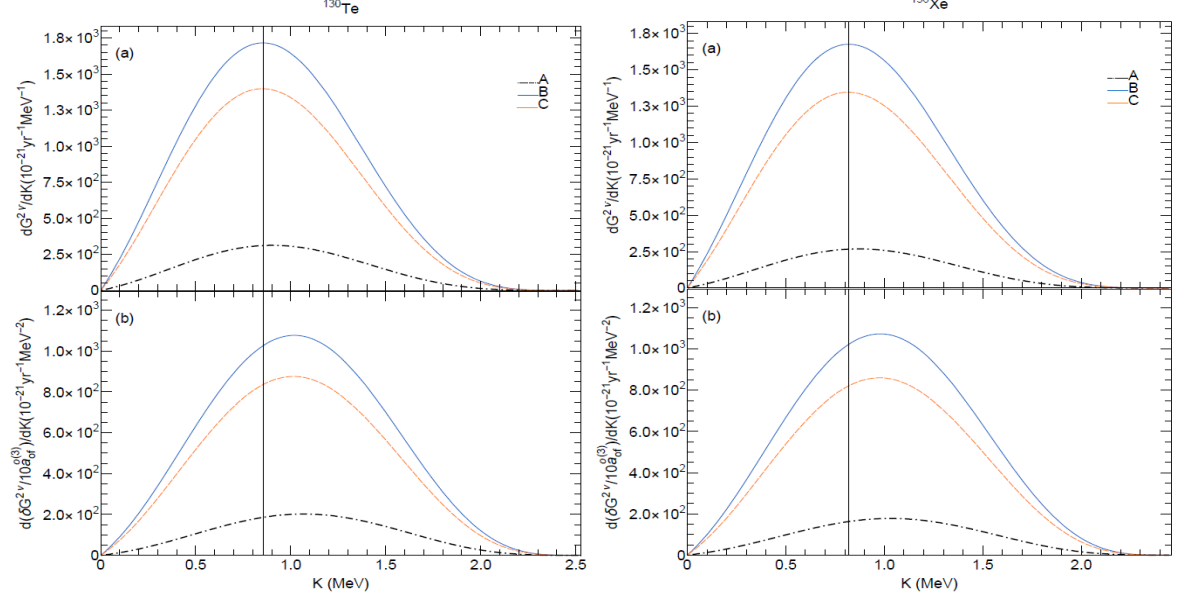
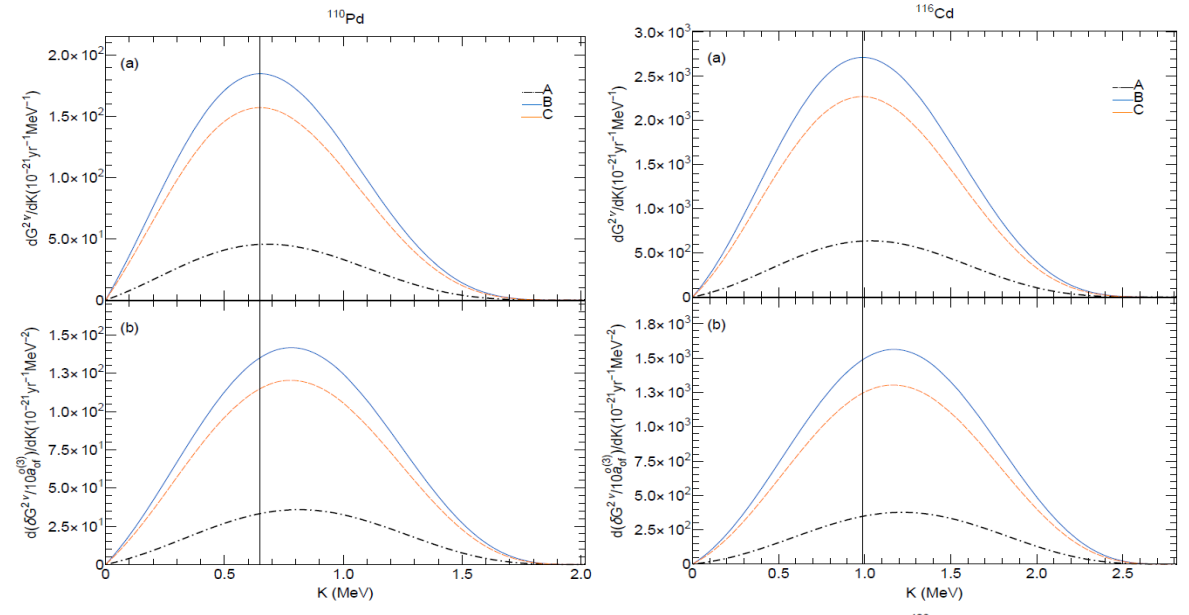


Figure 2. Summed energy spectra of electrons in the standard $2\nu\beta\beta$ decay (a) and their deviations due to LIV (b) for the nuclei ^{110}Pd , ^{116}Cd , ^{130}Te and ^{136}Xe .

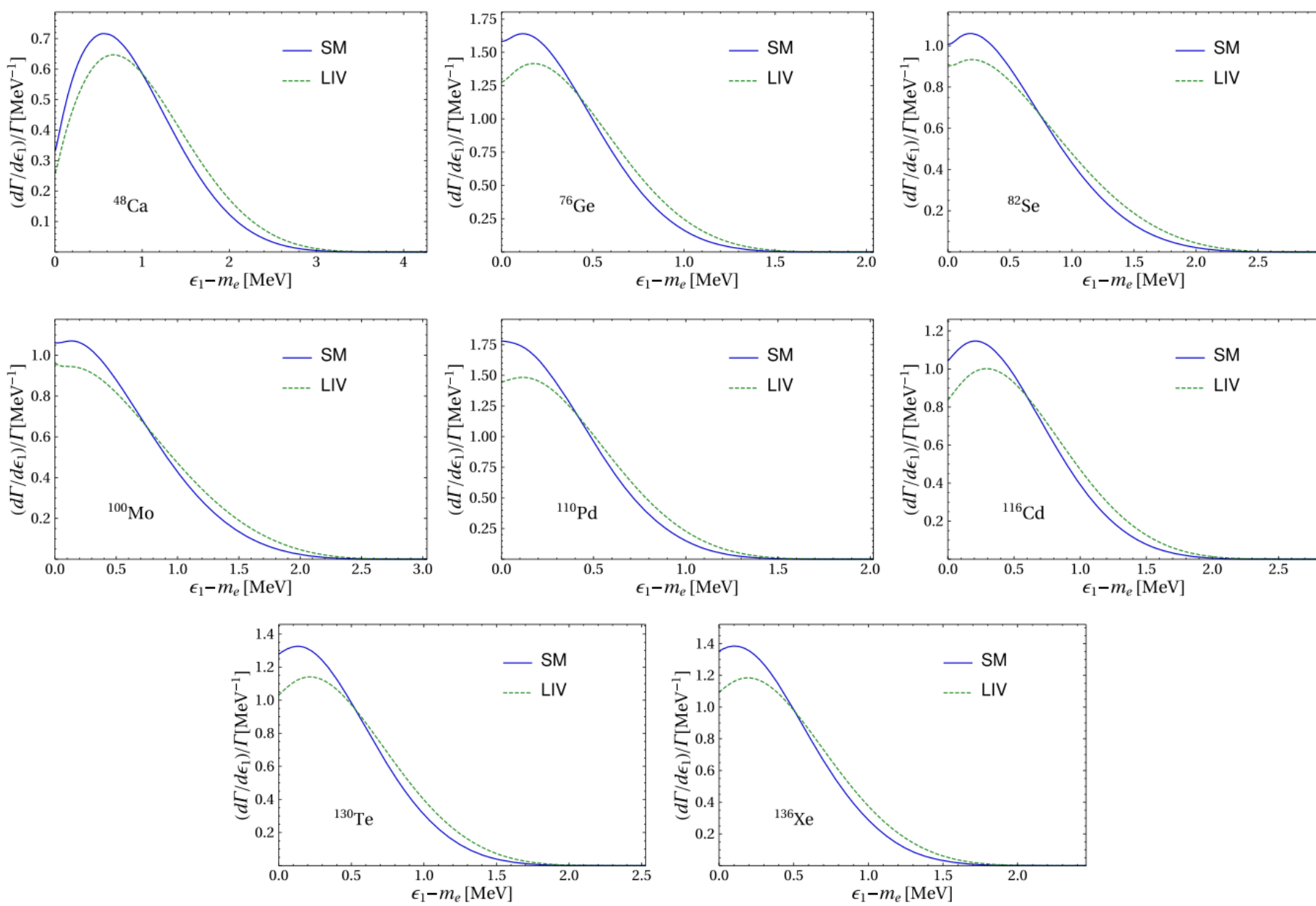


FIG. 1. Normalized $2\nu\beta\beta$ single-electron spectra within the SM with the solid line, and the first order contribution in $a_{\text{of}}^{(3)}$ due to LIV with the dashed line. See text for the assumption on the hypothesis used.

Niturescu, Ghinescu, Stoica
 PRD103(2021); 105(2022)

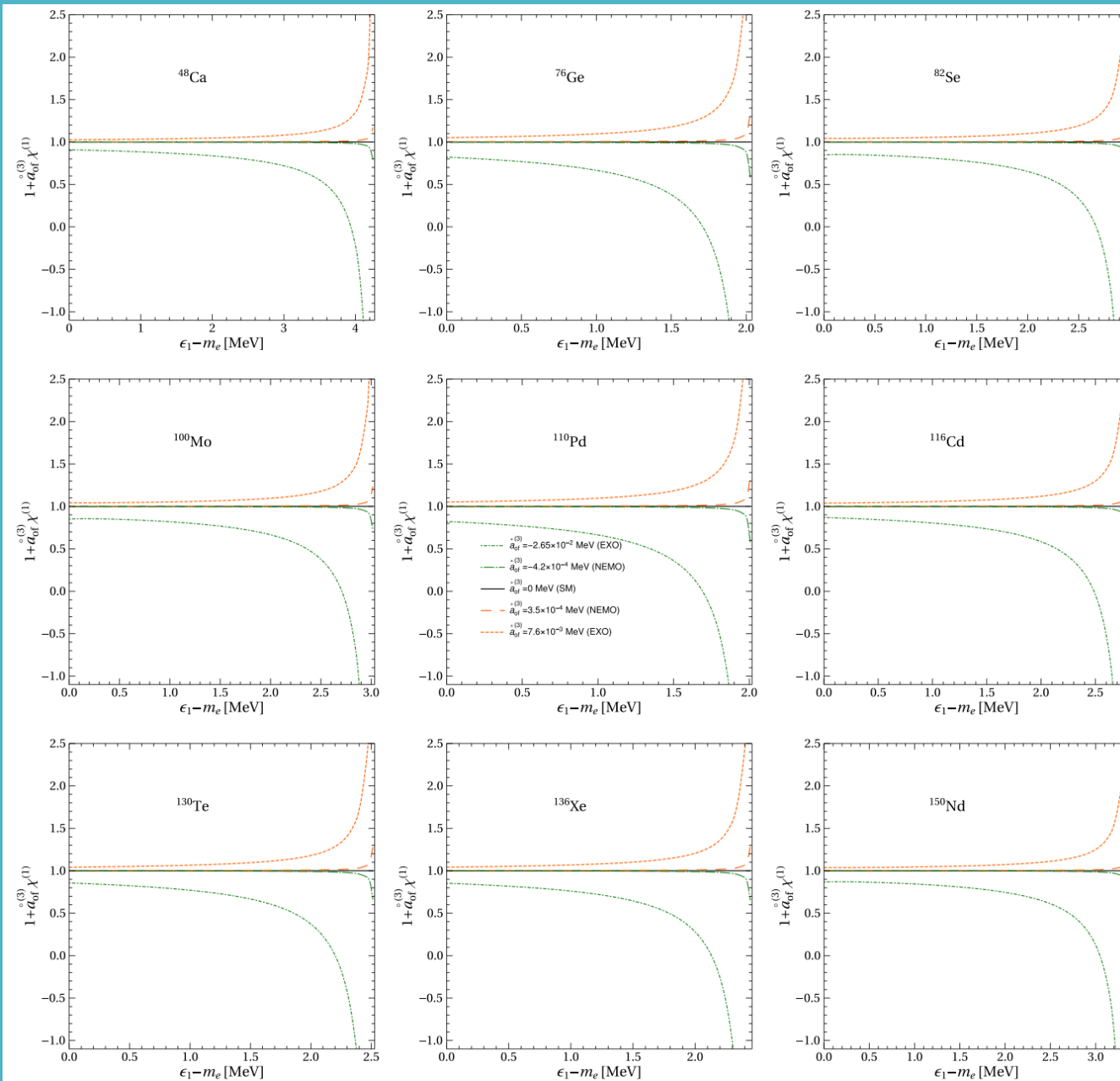


FIG. 3. The quantity $\chi^{(1)}(\epsilon_1)$ depicted for current limits of $a_{\text{of}}^{(3)}$ (dashed for upper limit and dot-dashed for lower limit). The solid line at $\chi^{(1)}(\epsilon_1) = 0$ represents the SM prediction.

Nitescu, Ghinescu, Stoica
PRD103(2021); 105(2022)

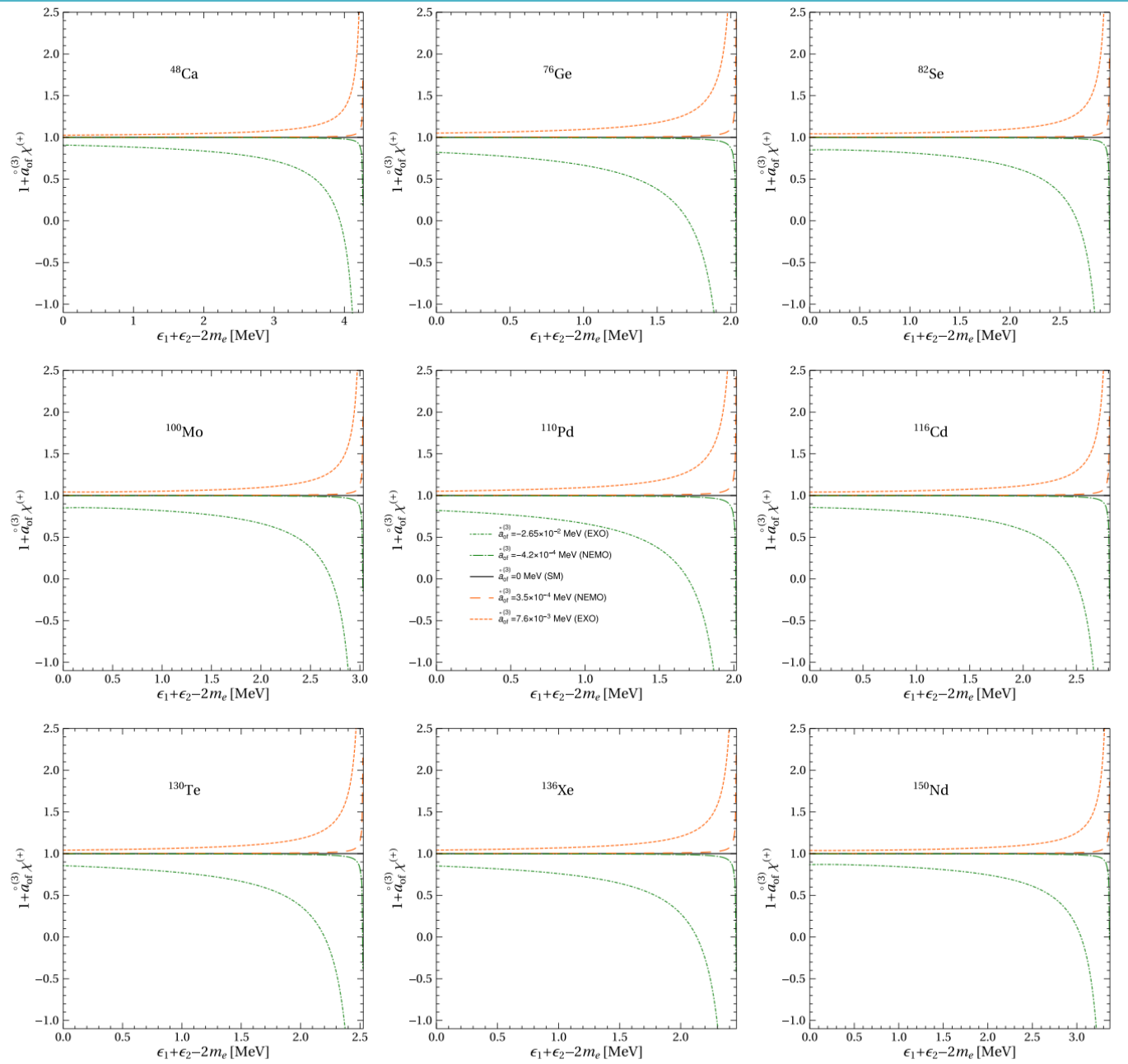


FIG. 4. The quantity $\chi^{(+)}(K)$ depicted for current limits of $a_{\text{of}}^{(3)}$. The same conventions as in Fig. 3 are used.

Nitescu, Ghinescu, Stoica
PRD103(2021); 105(2022)

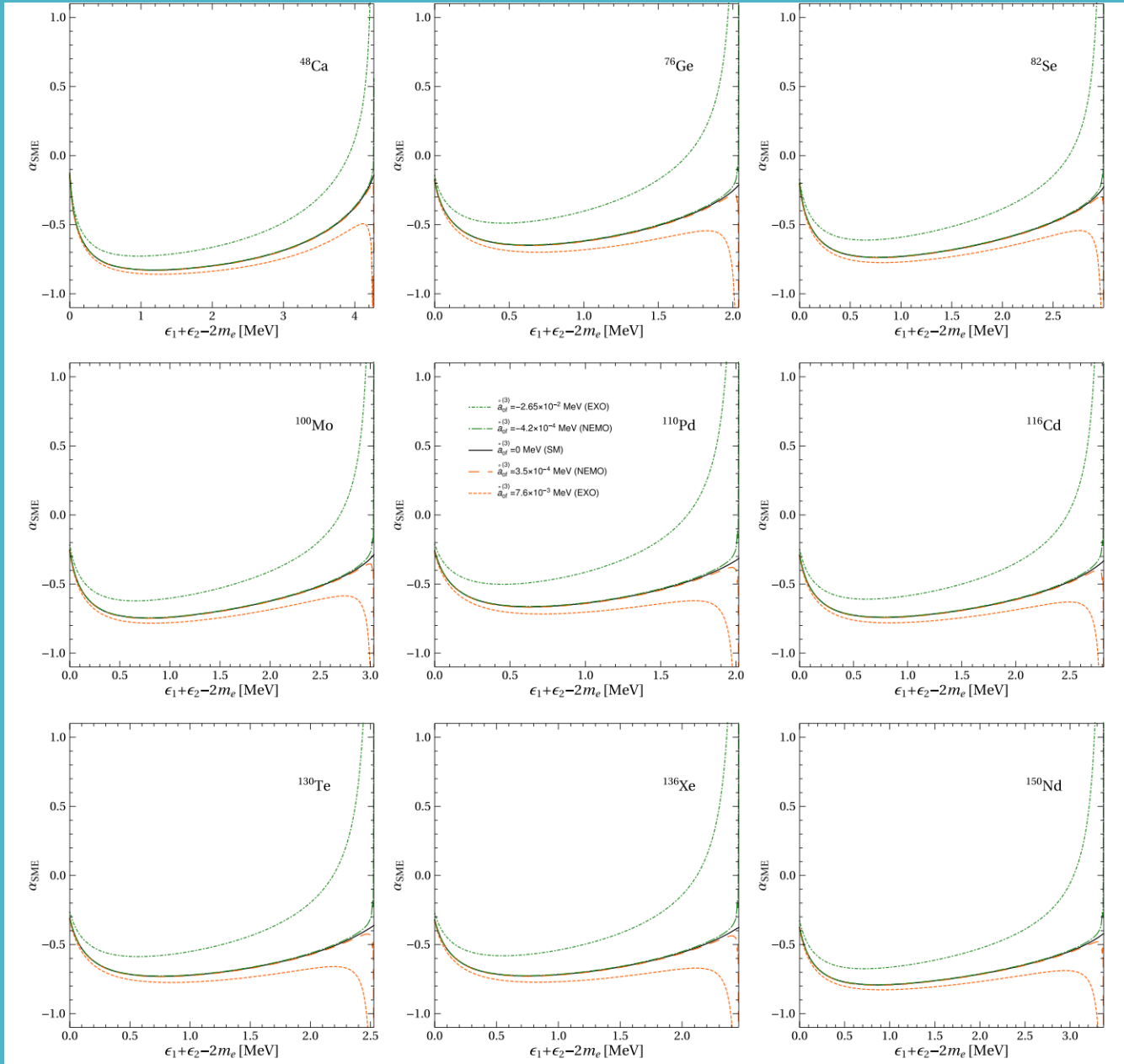


FIG. 5. The angular correlation spectrum plotted for the current limits of $a_{\text{of}}^{\circ(3)}$. The same conventions as in Fig. 3 are used.

Nitescu, Ghinescu, Stoica
PRD105(2022)

Angular correlation coefficient

$$\kappa_{\text{SM}}^{2\nu} = \frac{\Lambda_{\text{SM}}^{2\nu}}{\Gamma_{\text{SM}}^{2\nu}}$$

$$\kappa_{\text{SME}}^{2\nu} = \kappa_{\text{SM}}^{2\nu} + a_{\text{of}}^{(3)} \frac{\delta G_1^{2\nu}}{G_0^{2\nu}}$$

$$k_{\text{SME}}^{2\nu} = -0.6676 - 4.285 \times a_{\text{of}}^{(3)}$$

On the other hand, the angular correlation coefficient can be determined experimentally via forward-backward asymmetry

$$\mathcal{A}^{2\nu} \equiv \frac{\int_{-1}^0 \frac{d\Gamma^{2\nu}}{dx} dx - \int_0^1 \frac{d\Gamma^{2\nu}}{dx} dx}{\Gamma} = \frac{N_+ - N_-}{N_+ + N_-} = \frac{1}{2} k_{\text{SM}}^{2\nu}$$

where $x = \cos \theta_{12}$ and $N_-(N_+)$ are the $2\nu\beta\beta$ events with the angle θ_{12} smaller (larger) than $\pi/2$. For a number of $N = 5 \times 10^5$ events at NEMO-3 [12] and considering only the statistical errors, the angular correlation coefficient is measurable with the uncertainty $k_{\text{SM}}^{2\nu} = 0.6676 \pm 0.0027$. Without a statistically significant deviation from the SM expectation, we obtain a bound $|a_{\text{of}}^{(3)}| \lesssim 1.04 \times 10^{-3}$ MeV at 90% CL. This is only a rough estimation, and dedicated experimental analysis, including the systematic uncertainties, is necessary for a better one. We note that this estimation lies between the $a_{\text{of}}^{(3)}$ limits reported by NEMO-3 and EXO-200, which were obtained from the analysis of the summed energy spectra of electrons. We note here that if

in a future experiment the number of $2\nu\beta\beta$ events would increase by 3 orders of magnitude (as planned for example in the SuperNEMO experiment), our estimation yields $|a_{\text{of}}^{(3)}| \lesssim 3.3 \times 10^{-5}$ MeV at 90% CL, which is comparable with the limits obtained from tritium decay experiments [8]. Thus, we predict good perspectives for searching for LIV effects in future DBD experiments, due to the significant increase of statistics.

a comprehensive investigation of electron capture (EC) ratios spanning a broad range of atomic numbers. The study employs a self-consistent computational method that incorporates important atomic effects, including overlap and *exchange* corrections, as well as shake-up and shake-of effects within the EC formalism. The electronic wave functions are computed using the DHFS framework, which accurately describes electron screening and in the atomic structure.

In the case of EC and ECEC, energetic rearrangements processes are essential in the accurate measurement of the decay rates. Also, they are essential to be taken into account in the theoretical calculations and predictions of these processes.

- Great interest for theoretical description: program of systematically and precisely computation of EC processes

Applications

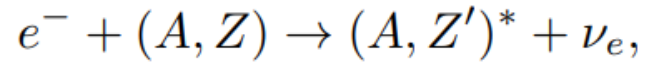
-radionuclide metrology and nuclear medicine (the relevance is that most Auger electrons emitted during EC processes possess kinetic energies in the range of a few keV, enabling precise deposition within a confined area, thus allowing targeted irradiation of tumour sites.)

- fundamental physics research like nuclear astrophysics & DM and DBD experiments

- specifically, in liquid Xenon experiments EC signals can produce misleading signatures that resemble with those of WIMPS and CE ν NS

- measurement of the 2 ν ECEC in ^{124}Xe : a critical background contribution emerges from ^{125}I EC, as its decay peak closely aligns with that of the 2 ν ECEC peak.

EC formalism



Transition probability per unit time

$$\lambda = \frac{G_\beta^2}{2\pi^3} \sum_x n_x C_x F_x S_x,$$

$$\lambda = \lambda_K + \lambda_{L_1} + \lambda_{L_2} + \dots$$

$$\frac{\lambda_{L_1}}{\lambda_K} = \frac{n_{L_1} q_{L_1}^2 \beta_{L_1}^2 B_{L_1} S_{L_1}}{n_K q_K^2 \beta_K^2 B_K S_K}.$$

Energetics

$$Q = q_x + \mathcal{M}_x^{(*)}(A, Z') - \mathcal{M}_{\text{gs}}(A, Z')$$

$$\begin{aligned} q_x &= Q - R_\gamma - [B_{\text{gs}}(Z') - B_x(Z')] \\ &= Q - R_\gamma - R_x. \end{aligned}$$

$$\begin{aligned} q_x &= \Delta M_{if} - R_\gamma + m_e - |E_x| \\ &= W_0 + W_x, \end{aligned}$$

Atomic effects

Exchange and overlap effects

$$\langle (m, \kappa)' | (m, \kappa) \rangle \neq 1.$$

Shake-up & shake-off processes

$$S_x = 1 + \sum_{m, \mu} P_{m\mu}$$

$$F_x = \frac{\pi}{2} q_x^2 \beta_x^2 B_x,$$

n_x = occupation number of the shell x ; C_x = NME; S_x = shake-up; shake-off effects; q_x = neutrino energy; β_x = Coulomb amplitude; B_x = overlap & exchange effects;

B

Working with atomic masses offers a clear advantage over nuclear masses. Nuclear masses are typically difficult to measure, while Q -values with small uncertainties can be obtained from the mass excesses provided in [31].

$$\begin{aligned} \left(\frac{d}{dr} + \frac{\kappa + 1}{r} \right) g_{n\kappa} - (W_{n\kappa} - V(r) + m_e) f_{n\kappa} &= 0, \\ \left(\frac{d}{dr} - \frac{\kappa - 1}{r} \right) f_{n\kappa} + (W_{n\kappa} - V(r) - m_e) g_{n\kappa} &= 0. \end{aligned}$$

$$V_{\text{ex}}(r) = \begin{cases} -\frac{3}{2}\alpha \left(\frac{3}{\pi}\right)^{1/3} [\rho(r)]^{1/3} & r < r_{\text{Latter}}, \\ -\frac{\alpha(Z_p - N_e + 1)}{r} - V_{\text{nuc}}(r) - V_{\text{el}}(r) & r \geq r_{\text{Latter}}. \end{cases} \quad (23)$$

$$V_{\text{el}}(r) = \alpha \int \frac{\rho(r')}{|\mathbf{r} - \mathbf{r}'|} d\mathbf{r}'.$$

$$\psi_{n\kappa m}(\mathbf{r}) = \begin{pmatrix} g_{n\kappa}(r) \Omega_{\kappa, m}(\hat{\mathbf{r}}) \\ i f_{n\kappa}(r) \Omega_{-\kappa, m}(\hat{\mathbf{r}}) \end{pmatrix}$$

The system of differential equations Eq. (18) is solved in the DHFS potential,

$$V_{\text{DHFS}}(r) = V_{\text{nuc}}(r) + V_{\text{el}}(r) + V_{\text{ex}}(r) \quad (23)$$

which is a sum of the nuclear, electronic and exchange potentials.

For the nuclear potential, $V_{\text{nuc}}(r)$, it is considered the electrostatic interaction of an electron at distance r with a spherical nucleus filled with protons following a Fermi distribution [31]

$$\rho_p(r) = \frac{\rho_0}{1 + e^{(r - R_n)/z}}, \quad (24)$$

where $R_n = 1.07A^{1/3}$ fm, $z = 0.546$ fm, and ρ_0 must be determined from normalization. Thus, the nuclear potential is

$$V_{\text{nuc}}(r) = -\alpha \int \frac{\rho_p(r')}{|\mathbf{r} - \mathbf{r}'|} d\mathbf{r}'. \quad (25)$$

Isotope	$E_{1s_{1/2}}$ (eV)				$E_{2s_{1/2}}$ (eV)				$E_{2p_{1/2}}$ (eV)			
	RLDA	KLI	DHFS	EXP	RLDA	KLI	DHFS	EXP	RLDA	KLI	DHFS	EXP
^7Be	-104.9	-131.0	-118.4	-115	-5.599	-10.259	-8.181	-9.322	-	-	-	-
^{41}Ca	-3929.4	-4052.6	-4015.1	-4041	-412.4	-439.2	-434.1	-441	-336.7	-364.4	-359.0	-353
^{54}Mn	-6397.0	-6552.8	-6510.9	-6544	-740.6	-772.3	-766.4	-775	-635.9	-669.6	-662.9	-656
^{55}Fe	-6963.3	-7126.1	-7083.4	-7117	-816.1	-849.0	-842.9	-851	-705.3	-740.4	-733.5	-726
^{125}I	-32765.9	-33162.8	-33165.0	-33176	-5067.8	-5151.9	-5162.2	-5195	-4761.3	-4852.3	-4857.7	-4858
^{138}La	-38483.4	-38922.4	-38944.2	-38928	-6132.4	-6225.7	-6242.2	-6269	-5790.8	-5891.5	-5902.8	-5894

TABLE I. The experimental binding energies (EXP) in comparison with DHFS, KLI and RLDA models described in the text. All binding energies are presented in eV for the inner shells of one light and a few medium and heavy neutral atoms in the ground state.

Isotope	$Q - R_\gamma(\text{keV})$ [28]	Type	Quantity	BS[28]	KLI[28] no vacancy	KLI[28] frozen orbitals	This work ^a	This work ^b	RD[62–70]
⁷ Be	861.89(7)	Allowed	λ_L/λ_K	0.105(8)	0.1606(41)	0.0509(20)	0.11054(3)	0.11053(3)	0.101(13)
⁴¹ Ca	421.64(14)	1st UF	λ_L/λ_K	0.09800(40)	0.10415(16)	0.09078(16)	0.1050(2)	0.1046(2)	0.102(10)
⁵⁴ Mn	542.2(10)	Allowed	λ_L/λ_K	0.11219(31)	0.10785(8)	0.09590(19)	0.1078(6)	0.1076(6)	0.1066(16)
			λ_K/λ	0.88419(34)	0.88623(10)	0.90005(21)	0.8869(5)	0.8870(5)	0.8896(17)
⁵⁵ Fe	231.21(18)	Allowed	λ_L/λ_K	0.11629(31)	0.11236(8)	0.10073(20)	0.1125(3)	0.1121(3)	0.1110(15)
			λ_M/λ_K	0.01824(12)	0.019390(32)	0.014824(45)	0.01918(4)	0.01909(5)	0.01786(29) ^c
			λ_M/λ_L	0.1568(11)	0.17257(31)	0.14716(49)	0.1705(4)	0.1704(4)	0.1556(26) ^c
¹⁰⁹ Cd	127.1(18)	Allowed	λ_K/λ	0.8148(14)	0.8097(11)	0.8164(12)	0.807(7)	0.810(7)	0.812(3)
			λ_{L+}/λ_K	0.2274(12)	0.2350(11)	0.2250(12)	0.2390(101)	0.2344(101)	0.2315(8)
¹²⁵ I	150.28(6)	Allowed	λ_K/λ	0.79927(41)	0.79798(7)	0.80376(23)	0.7952(2)	0.7983(18)	0.8011(17)
¹³⁸ La	312.6(3)	2nd UF	λ_L/λ_K	0.3913(25)	0.4077(15)	0.4242(49)	0.420(3)	0.409(7)	0.432(6)
			λ_M/λ_K	0.0965(9)	0.09908(41)	0.1002(11)	0.1025(8)	0.100(2)	0.102(3) ^c
			λ_M/λ_L	0.2465(20)	0.2430(22)	0.2362(24)	0.244(1)	0.244(1)	0.261(9) ^c

- Investigation of the exchange effect between the final atom's bound electrons and those emitted in the allowed β decay of the initial nucleus. This refers to the interchange of the emitted electrons from different β transitions with the bound electrons from only the 1s orbital.
- The importance of the exchange corrections was first proved for tritium β decay and then confirmed for other nuclear β decays (e.g. the allowed β transitions of ^{14}C , ^{35}S , ^{106}Ru and the non-unique first forbidden β transition of ^{241}Pu . The β spectrum better agrees with the experimental one when exchange corrections are included (the effect is more pronounced at low energies)
- The exchange effect is also important for excluding background β events in experimental analysis, e.g., LUX-ZEPLIN, XENON (1T&nT) experiments (in this regard in case of the unique first forbidden transition of ^{85}Kr and non-unique first forbidden transitions of ^{212}Pb).
- First, we calculate the exchange effect for the low-energy β transitions in ^{14}C , ^{45}Ca , ^{63}Ni , and ^{241}Pu , recently investigated in the literature.
- Next, we compute the total exchange correction for a large number of β emitters, with $Z \in (1-102)$

Exchange corrections

$$\frac{d\Gamma^{s_{1/2}}}{dE_e} \Rightarrow \frac{d\Gamma^{s_{1/2}}}{dE_e} \times (1 + \eta_1^T(E_e))$$

$$\frac{d\Gamma^{p_{3/2}}}{dE_e} \Rightarrow \frac{d\Gamma^{p_{3/2}}}{dE_e} \times (1 + \eta_2^T(E_e))$$

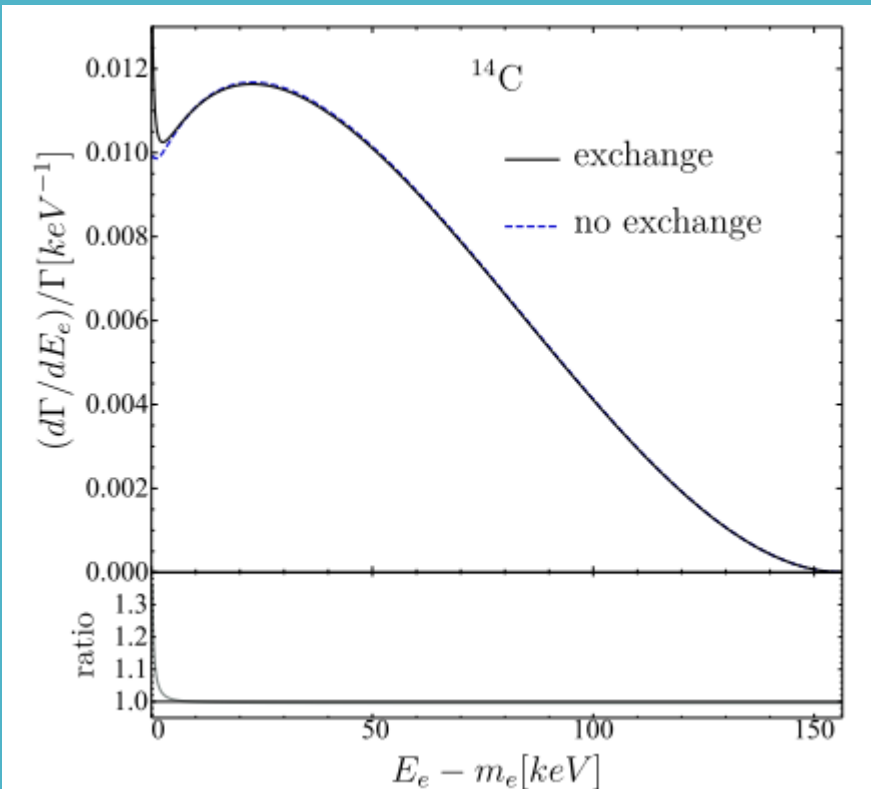
$$\eta_\kappa(E_e) = \sum_n \eta_{n\kappa} + f_{|\kappa|} \sum_{\substack{n,m \\ n \neq m}} T_{n\kappa} T_{m\kappa}$$

$$\eta_\kappa(E_e) = \sum_n \eta_{n\kappa} + (1 - f_\kappa) \sum_{\substack{n,m \\ n \neq m}} T_{n\kappa} T_{m\kappa}$$

$$T_\kappa = \sum_{(n\kappa)'} T_{n\kappa} = - \sum_{(n\kappa)'} \frac{\langle \psi'_{E_e\kappa} | \psi_{n\kappa} \rangle}{\langle \psi'_{n\kappa} | \psi_{n\kappa} \rangle} \frac{g'_{n,\kappa}(R)}{g'_\kappa(E_e, R)}, \quad (1)$$

$$\langle \psi'_{E_e\kappa} | \psi_{n\kappa} \rangle = \int_0^\infty r^2 g'_\kappa(E_e, r) g_{n,\kappa}(r) dr$$

$$+ \int_0^\infty r^2 f'_\kappa(E_e, r) f_{n,\kappa}(r) dr.$$



- A key ingredient of this work was to ensure the orthogonality between the continuum and bound electron states, in the potential of the final atom, by modifying the last iteration of the DHFS self-consistent method. After imposing the orthogonality, we found considerable differences in magnitude and energy dependence compared to previous results.
- Total exchange effect: presents a completely different energy dependence and the orthogonality of the wave functions strongly also influences its magnitude. The downturn observed at very low energy in the case of non-orthogonality between the bound and continuum electron states disappears when the orthogonality is assured. Therefore, the calculation of the exchange correction for ultra-low Q-value β transitions should address the orthogonalization between the continuum and bound wave functions for the final atom.
- extending the study to a large range of isotopes, we provide an analytical expression of the total exchange correction for each atomic number for easy implementation in experimental investigations.

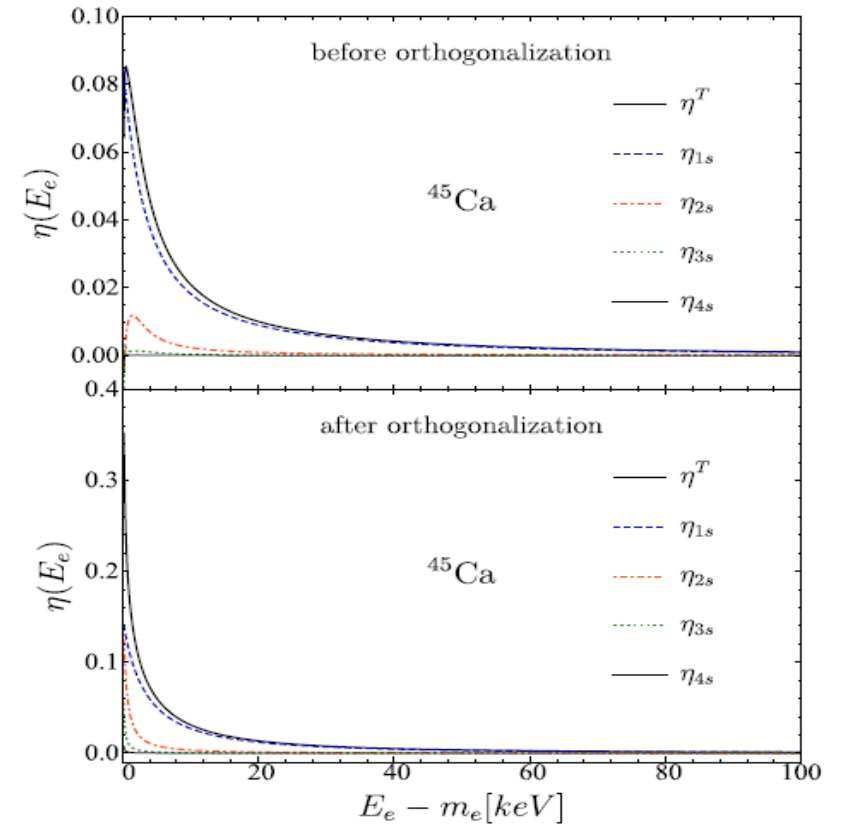


FIG. 4. The total exchange correction and the partial contributions from all occupied $s_{1/2}$ orbitals as functions of the kinetic energy of the electron emitted in the β -decay of ^{45}Ca . The top figure is obtained with non-orthogonal continuum and bound states of the final atom (see text). In the bottom part the orthogonality is ensured by the modified DHFS self-consistent method.

Conclusions

- Beta decay and double-beta decay continuous to be current topics of great interest for several domains of physics: atomic, nuclear, particle, astro-physics and have also a broad potential to explore different aspects of BSM physics : neutrino properties, conservation and symmetry laws, constrain different scenarios for $0\nu\beta\beta$ decay .
- I presented a brief review on some recent results related to the computation of the kinetic part of the decay rates of these weak processes: obtaining of accurate electron wave functions, and then predictions of electron and angular correlation spectra and computation of several atomic effects.
- These calculations were applied to the investigation of LIV in $2\nu\beta\beta$ decay and description of EC processes
- We provide the formalism for investigating LIV effects in summed and single energy electron spectra and angular correlation and show that other possible signatures may also be observed in these spectra. Next, we propose an alternative, new method for constraining the $a^{(3)}_{of}$ coefficient from the measurement of the forward-backward asymmetry of the emitted electrons.
- EC processes are of great interest both for practical applications in nuclear metrology and nuclear medicine and for providing information about the background composition in DM and DBD experiments.
- I presented calculations that provide a complete description of these processes , including obtaining precise electron w.f. for continuous and bound states, and with inclusion of several, essential atomic corrections: FNS, screening, exchange and overlap, shake-up and shake off effects.

Thank You

Team

Andrei Neacsu (CIFRA)

Ovidiu Nutescu (CIFRA, Bratislava)

Stefan Ghinescu (CIFRA)

Vasile Sevestrean (CIFRA)

Sabin Stoica (CIFRA)

Fedor Simkovic (Bratislava)

R. Dvornick'y (Bratislava)

Jouni Suhonen (Jyvaskyla, CIFRA)

Jenni Kotila (Jyvaskyula, CIFRA)

Mihai Horoi (CMU, CIFRA)

Project NEPTUN (*Neutrino Properties Through Use of Nuclei*) (CIFRA-Jyvaskyula-CMU)

PI: Jouni Suhonen